Journal of Cellular Biochemistry 76:217–230 (1999)

Effects of Static or Dynamic Mechanical Stresses on Osteoblast Phenotype Expression in Three-Dimensional Contractile Collagen Gels

Omar Akhouayri, Marie-Hélène Lafage-Proust, Aline Rattner, Norbert Laroche, Anne Caillot-Augusseau, Christian Alexandre,* and Laurence Vico

Laboratoire de Biologie et Biochimie du Tissu Osseux, Institut National de la Santé et de la Recherche Médicale (INSERM) E9901, GIP Exercice, 42023 Saint-Etienne, France

Abstract Studies performed at tissular (three-dimensional, 3-D) or cellular (two-dimensional, 2-D) levels showed that the loading pattern plays a crucial role in the osteoblastic physiology. In this study, we attempted to investigate the response of a 3-D osteoblastic culture submitted to either no external stress or static or dynamic stresses. Rat osteosarcoma cells (ROS 17/2.8) were embedded within collagen type I lattices and studied for 3 weeks. Entrapment and proliferation of cells within the hydrated collagen gel resulted in the generation of contractile forces, which led to contraction of the collagen gel. We used this ability to evaluate the influence of three modes of mechanical stresses on the cell proliferation and differentiation: (1) the freely retracted gels (FRG) were floating in the medium, (2) the tense gels (TG) were stretched statically and isometrically, with contraction prevented in the longitudinal axis, and (3) the dynamic gels (DG) were floating gels submitted to periodic stresses (50 or 25 rpm frequency). Gels showed maximum contraction at day 12 in 50 rpm DG, followed by 25 rpm DG, then FRG (88%, 81%, 70%, respectively) and at day 16 in TG (33%). The proliferation rate was greater in TG than in FRG (+52%) but remained low in both DGs. Gel dimensions were related to the collagen concentration and on a minor extent to cell number. Cells in DG appeared rounder and larger than in other conditions. In TG, cells were elongated and oriented primarily along the tension axis. Scanning electron microscopy (SEM) showed that tension exerted by cells in TG led to reorientation of collagen fibers which, in turn, determined the spatial orientation and morphology of the cells. Transmission electron microscopy (TEM) performed at maximum proliferation showed a vast majority of cells with a distended well-developed RER filled with granular material and numerous mitochondria. Alkaline phosphatase activity peaked close to the proliferation peak in FRG, whereas in TG, a biphasic curve was observed with a small peak at day 4 and the main peak at day 16. In DG, this activity was lower than in the two other conditions. A similar time course was observed for alkaline phosphatase gene expression as assessed by Northern blots. Regardless of the conditions, osteocalcin level showed a triphasic pattern: a first increase at day 2, followed by a decrease from day 4 to 14, and a second increase above initial values at day 18. Microanalysis-x indicated that mineralization occurred after 14 days and TEM showed crystals within the matrix. We showed that static and dynamic mechanical stresses, in concert with 3-D collagen matrices, played a significant role on the phenotypic modulation of osteoblast-like cells. This experimental model provided a tool to investigate the significance and the mechanisms of mechanical activity of the 3-D cultured osteoblast-like cells. J. Cell. Biochem. 76:217–230, 1999.

Key words: ROS 17/2.8; type I collagen; ultrastructure; proliferation; alkaline phosphatase; osteocalcin; mineralization

Mechanical loads induce strain and/or shear stresses in bone that can be detected by bone cells. Tissular responses such as functionally isolated, externally loadable, avian ulna preparation [Lanyon and Rubin, 1984] showed that dynamic loads not only prevent the resorption that normally accompanies reduced loading, but also result in increase in bone formation proportional to the peak strain magnitude [Rubin and Lanyon, 1985]. By contrast, static load applied continuously in this system produced no effect [Lanyon and Rubin, 1984]. Other studies using the in vivo 4-point bending model in rat tibiae confirmed that static load does not play a significant role and that bone formation

Grant sponsor: European Space Agency (ESA) European Research in Space and Terrestrial Osteoporosis (ERISTO) project.

*Correspondence to: Christian Alexandre, LBBTO, E9901, GIP Exercice Faculté de Médecine, 15 rue Ambroise Paré, 42023 St. Etienne, France. E-mail: vico@univ-st-etienne.fr

Received 19 February 1999; Accepted 28 June 1999

is threshold-driven and dependent on strain rate, amplitude, and duration of loading [Forwood and Turner, 1995]. However, the inevitable static load related to body weight is important in maintaining the structural competence of the skeleton, as suggested by the bone loss measured mainly in weight-bearing bones after microgravity exposure [Vico et al., 1998]. Because of the well-documented strain-related changes in the osteoblastic and osteocytic cells, a number of model systems for in vitro studies have been developed in which the responses to physical forces can be explored at various levels. These different techniques included hydrostatic pressure, stretching, or bending of the cell substratum and/or fluid shear stresses [see Duncan and Turner, 1995, for review]. These models have produced a wide range of results in proliferation and differentiation responses, depending on the cell lines, models used, and observation timing (short term vs long term) [Duncan and Turner, 1995], making correlation between in vitro and in vivo studies difficult. Most in vitro models are able to produce intermittent rather than continuous mechanical stresses. Furthermore, it appeared that the condition of dynamic mechanical regimen might be different for promoting cell division and for other cell functions. Very few studies have compared static versus dynamic forces in vitro. However, one example is provided by rat osteosarcoma ROS 17/2.8 cells, which responded differently when submitted to gravitational stress (i.e., consecutive periods of 2G and OG, provided by parabolic flights) [Guignandon et al., 1997a], as compared with continuous microgravity exposure as provided by space flight [Guignandon et al., 1997b].

In the present study, we developed a three-dimensional (3-D) model system of culture that should (1) provide a situation closest to in vivo conditions, (2) permit study of one cell type independently from other factors acting on the bone cells in situ, and (3) permit comparison of the effects of either static or dynamic forces on the behavior of osteoblast-like cells in the same culture system. Indeed, experiments carried in 3-D environments provided improvements, as compared with the classic 2-D in vitro culture system. For example, alginate beads promoted enrichment of osteoblasts in primary cultures [Majmudar et al., 1991]. Comparing phenotypic differentiation in Saos-2 human osteoblastic cells cultured either in 2-D or 3-D, Masi et al. [1992] observed that only the 3-D model allowed cells to synthesize osteocalcin without any other induction. It was concluded that 3-D culture is an adequate model for investigating osteoblastic cells through their differentiation process. In view of these findings, 3-D cell culture approaches were developed, including osteoblast-like cell growth in methylcellulose [Ernest et al., 1987], cell cultures with 3-D carriers such as Fibro-Cel carriers in nonwoven polyester fabric [Benayahu et al., 1994] beads [Granet et al., 1998], collagen sponges [Heermeier et al., 1995], and denatured collagen gels [Casser-Bette et al., 1990]. Moreover, the expression of the final stages of osteogenic differentiation in vitro implies the 3-D production of an osteoid-like matrix. In conventional 2-D cultures, mineralizing osteoid is only observed in multilayered structures that form nodules after extended period of time [Bellows et al., 1986; Benayahu et al., 1989].

Like fibroblastic cells, fetal rat calvaria cells seeded in a 3-D collagen gel matrix were shown to contract the gel gradually [Bellows et al., 1981]. It appeared to us that, under these circumstances, osteoblastic cells that share some fibroblastic features could also form extensions, collect collagen, and contract the matrix structure, providing an index of the cell population behavior. We intended to use this property to evaluate the influence of different mechanical strains.

Our first aim was to study the influence of a 3-D culture system on both proliferation and differentiation of rat osteosarcoma cells (ROS 17/2.8) that have well-defined osteoblastic properties. As the 3-D structural substrate, we chose type I collagen gels that provided a filamentous network. Indeed, it has been indicated that type I collagen, the major component of bone extracellular matrix, is fundamental for the expression of the osteoblast phenotype and formation of the mineralized matrix in nontransformed cells [Lynch et al., 1995]. Our second aim was to examine the effects of physical stimuli in vitro in this type of spatial culture environment. We investigated the effects of three modes of tensile stress on lattices: isotonic (control), isometric (static stress), and periodic (dynamic stress). Morphological (i.e., structural and ultrastructural), biochemical, and transcriptional alterations as well as gel contraction under such conditions were evaluated. Furthermore, the mineralization pattern

was evaluated using electron microscopy and X-ray microanalysis.

MATERIALS AND METHODS

Cell Culture

Osteosarcoma cells ROS17/2.8 derived from Wistar stump rat [Majeska et al., 1980] were well-defined cells, presenting the same characteristics exhibited by matured osteoblasts (alkaline phosphatase [ALP], osteocalcin, and the ability to mineralize). These cells were seeded in tissue culture T75-flask (Elvetec Services, Venissieux, France) in Dulbecco's modified Eagle's medium (DMEM) (Boehringer, Gagny, France) supplemented with 10% fetal calf serum (FCS) (Boehringer, Gagny, France), 2 mmol/L L-glutamine and 1% antibiotics (10,000 U of penicillin and 10 mg streptomycin; Sigma Chemical Co., St Quentin Fallavier, France). The cultures were incubated in a humidified atmosphere of 5% CO_2 in air at 37°C (Incubator Queue, France). At confluence, cells were trypsinized with 1× trypsin-EDTA (Sigma, France) and were mixed to collagen plated at a density of 8×10^4 cells per ml within collagen gels.

Preparation of 3-D Culture

Collagen gels were prepared by mixing type I collagen from bovine skin dissolved in 0.012 N HCl (Vitrogen 100—3 mg/ml Collagen GmbH, Germany), FCS 10%, antibiotics 1%, 5× DMEM 20% and cell suspension. The 5× DMEM, FCS, antibiotics, and ROS17/2.8 cells were mixed and added to Vitrogen neutralized with 1 N NaOH 0.4%. The volume of collagen was adjusted to obtain a final concentration of 2 mg/ml and was adjusted to physiological ionic strength and neutral pH; 2 ml of this solution was mixed with 16×10^4 cells and poured in each well (8-well rectangular multidish, 3.2×2.7 cm^2 per well; NUNC, Naperville, IL). Gelation was completed after 4 h at 37°C. Then, culture medium containing DMEM supplemented with 10% FCS, 2% L-glutamine, 1% antibiotics, 50 mg/ml L-ascorbic acid and 5 mM β-glycerophosphate were added and replaced every other day. Three modes of mechanical stress-loading regimens were applied:

The freely retracted gels (FRG) were treated as follows: after gelation, a sterile needle was used to cut the gels at the periphery of the dishes, allowing the gel to float and shrink with no restriction. This condition was used as an isotonic control tissue.

The tense gels (TG) were obtained by pouring the mixture (collagen and cells) into plastic wells in which small sterile Velcro™ ribbons (2×2.7 mm^2) were previously fixed with a silicone sealant on the small sides of the rectangular dishes. This permitted anchoring the gel extremities along the small culture dish sides, with the large sides unstuck as previously described. As far as contraction occurred, the gel was statically and isometrically stressed between the two Velcro™.

The dynamic gels (DG) were floating gels submitted to periodic stress. Culture dishes were placed on the plate of a Belly Dancer (IKAr-Schüttler MTS2, Staufen, Germany). The heart of the drive is a strong nonblocking external rotor-type capacitor motor. The speed of motor is constant as controlled by apto-electronic measurements. Shaking of the platform is driven by an eccentric with a 3-mm lift (peak to peak). The rotary movement of the eccentric is transmitted to the platform by a strong ball-bearing. Three tubular connecting pieces prevent the platform from turning. Contrary to traditional one-point holders, these silicon connecting pieces fit symmetrically to the center of rotation, ensuring an uniform horizontally circular movement at each point of the platform. The frequency of rotation was 25 and 50 rotations per minute (rpm).

Electron Microscopy

The culture medium was washed out with 1× phosphate-buffered saline (PBS) without calcium and magnesium. At different time intervals (days 12, 14, and 16), collagen gels were fixed with 4% glutaraldehyde in 0.2 M cacodylate buffer for 1 h 30 min at 4°C and then postfixed in 2% osmium tetroxide (OsO_4) in 0.3 M cacodylate buffer for 1 h at 4°C. The osmium precipitates were then washed out from collagen gels with 1× PBS.

For transmission electron microscopy (TEM), OsO_4-fixed samples were dehydrated in an ethanol series and embedded in Epon (Epon 812, Taab, England). Thick sections of about 80-nm thickness were cut perpendicularly to, or in parallel with, the surface of the collagen gels by an ultramicrotome (MT 600 XL Microm) and observed under a Hitachi 800 electron microscope at 75 kEv.

For scanning electron microscopy (SEM), OsO_4-fixed samples were dehydrated in an acetone series and critical-point dried (E 3000 critical-point dryer), mounted on slide, sputtered with gold, and viewed with an JSM 840 Scanning Electron Microscope (JEOL, Tokyo, Japan) at 15 kEv. Energy dispersive X-ray microanalysis was also performed using the same apparatus equipped with a TRACOR® Si(Li) energy-dispersive X-ray spectrometer. The operating conditions were as follows: accelerating voltage: 15 kV, beam current: 1 nA, takeoff angle: 40° Spectra were collected by point electron beam at ×400 for 50-s live time. The Ca/P molar ratio was determined.

Contraction Determination

Collagen gel contraction was measured at multiple time points, including 0, 2, 4, 6, 8, 10, 12, 14, and 16 days, using a measuring rod. At each time point, the gel width in the centrum of the well was measured 10 times.

Cell Number

In order to harvest cells, collagen gels were solubilized by 0.2% collagenase digestion for 20 min (2 mg/ml in DMEM, type IA (Sigma Chemical Co, St. Louis, MO) at 37°C with mild agitation. The number of cells in collagen gels was determined at various time points by direct counting with a hemocytometer. At each time point, the cell number was counted four times using the Trypan blue dye exclusion method in order to count only viable cells.

Collagen Quantification

In the collagen lattices, the amount of hydroxyproline was measured using Stegeman's method after hydrolysis [Stegeman et al., 1958] and used as an index of collagen concentration. Basal control analysis was performed on initial mixture without cells.

Determination of Alkaline Phosphatase Activity

After cell counts, the cell suspension was centrifuged and solubilized in 0.1% Triton X-100 and then assayed for protein content and ALP activity. Protein concentration was determined by a microprotein assay [Bradford et al., 1976], using bovine serum albumin (BSA) to construct standard calibration curves; 100 µl of the cell homogenate was mixed with 4 ml of final Coomassie blue solution at dark room for 10 min, and the absorbance was read in a spectrophotometer (940 KONTRON) at 595 nm, using a blank as a reference and the protein concentration determined on the basis of the calibration curve.

ALP was determined by measurement of the hydrolysis of PNP-p. The assay mixture consisted of 100 µl cell homogenate and 900 µl reaction mixture (2 mM PNP-p, 2 mM $MgCl_2$, 2-amino-2-methyl-1-propanol 95% pH = 10.5), the reaction was initiated by the addition of the cell extract, and absorbance at 412 nm was measured after 20 min. ALP was expressed as mmol P_i per mg of protein.

Osteocalcin Assay

After 24 h of incubation, 1 ml of serum-free medium was harvested in each condition every day. Osteocalcin (OC) was assayed in duplicate by radioimmunoassay (RIA) [Caillot et al., 1996], using a rabbit anti-Oc polyclonal immunoserum, depending on the epitopes recognized by the antibody to the intact molecules (Elsa-ostnat [Cis]) (CIS bio International society).

Northern Blot Analysis of Total Cellular RNA

Total RNA was isolated according to the guanidinium-isothiocyanate-acid-phenol method, as described by Chomczynski and Sacchi [1987]. Briefly, 8 collagen gels from each time point were pooled and incubated for 30 s in 2 ml of a solution consisting of guanidinium isothiocynate and mercaptoethanol (Roti®-Quick, Carl Roth-Sochiel, Lauterbourg, France; solution 1). Total RNA was extracted with 2.6 ml of a solution of chloroform/phenol (solution 2), added to the homogenates. After centrifugation, the RNA in the supernatant was precipitated with isopropanol (solution 3), centrifuged at 10,000*g*, resuspended in 600 µl of solution 1 and 600 µl of solution 3, centrifuged again at 10,000*g*, washed with 70% ethanol, air-dried, and dissolved in 200 µl of 0.1% DiEthyl PyroCarbonate (DEPC, Sigma, France). Total RNA was quantitated by measuring the absorbance at 260 nm, using a spectrophotometer (940 KONTRON).

For Northern blotting, 30 µg of total RNA was loaded into 3.4% formaldehyde and 1% agarose gel and transferred to a Membrane Appligen Neutral (Appligen Oncor®, France) in 10× SCC. The bound RNA was immobilized under ultraviolet (UV), prehybridized and hybridized at 42°C in 50% formamide, 25% SCC

20×, 0.5% SDS 20%, 10% Denhardt's solution and 10% salmon sperm DNA.

Rat ALP complementary DNA (cDNA) inserts was kind gift of G. Rodan (Merck, West Point, PA). The probes were labeled with ^{32}P deoxy-CTP, using random primer nucleotides (Nonaprimer Kit I, Appligen Oncor®, Illkirch, France). After hybridization with labeled AP and OC cDNA, the membrane was washed 3 times for 5 min with 0.5% sodium dodecyl sulfate (SDS) 20%, 0.5% SCC 20× at room temperature and 30 min with 0.5% SDS 20%, 0.5% SCC 20× at 65°C. The membrane was exposed to X-ray Kodak film for 10 days at −80°C.

Calcium Determination

Every day between days 2 and 18, two lattices per group were washed with 1× PBS, digested with 0.2% collagenase (w/v) for 15 min at 37°C, centrifuged for 5 min, and the pellet was dissolved in 5% perchloric acid. One lattice without cells was also harvested every day as the control. Quantitation of total calcium was accomplished by a method using a flame atomic absorption spectrometer (Eppendorf FCM6341).

RESULTS

Contraction of the Gels

Contraction data are presented in Figure 1. After a latency period, contraction occurred first in DG (50 rpm induced more contraction than 25 rpm), then in FRG, and last in TG. Maximum of contraction occurred between the 4th and 6th day of culture in every conditions, with the strongest effect in DG. At day 12, contraction reached 88%, 81%, and 70% of initial volume for dynamic gels 50 rpm, and 25 rpm, FRGs, respectively. For tense gels, it reached 33% at day 16.

Cellular Morphology

We examined the morphology of ROS17/2.8 cells cultured in type I collagen gels. In each condition (TG, DG, FRG), the cells began to gather at day 2 and form a mesh-like structure permitting gel contraction. Freely retracted lattices showed round-shaped cells with extended pseudopods. Collagen fibers were more abondant around cell clusters. Pseudopods were multidirectional. Lattices retracted according to well shape, remaining rectangular. Cells in dynamic gels were also round shaped and presented multidirectional pseudopods. However, cells appeared larger, and pseudopods were less numerous than in FRG. In tense gels, most of the cells were spindle shaped. Both cells and collagen fibers were oriented according to the lattice long axis. Nevertheless, some retraction was observed in the gel centrum.

Intracellular and Extracellular Ultrastructure at Electron Microscopic Level

As observed with TEM, during exponential proliferation, the cytoplasm was rich in mitochondria, polysomes, and particularly large RER cisternae and contained a well-developed Golgi apparatus. The cells presented characteristics of active cells under protein synthesis. Vesicles were found in the outer cytoplasm and opened into the extracellular space. Gap junc-

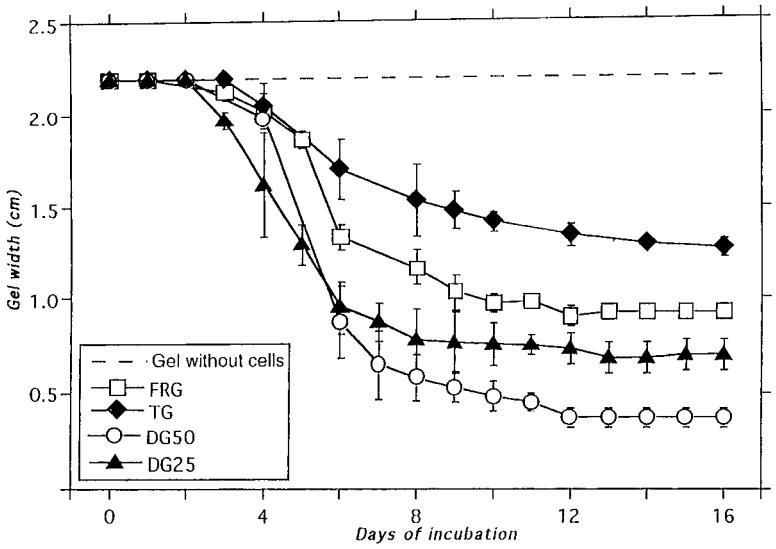

Fig. 1. Contraction of ROS17/2.8 cells. Populated type I collagen gels submitted to different kind of stresses. Values are means ±SD of 10 determinations.

tions were also found in bridging cells. Short fibrils and a nonfibrillar material were occasionally seen close to the osteoblast-like cells. At the end of the culture, numerous large vacuoles and nuclei that were not well delimited were seen. SEM analysis showed FRG or DG round-shaped cells included in collagen fibers mesh-like structure (Fig. 2). In TG, collagen fibers were oriented after tension axis, in contrast to the random orientation of collagen fibers observed in FRG and DG.

Cell Growth

Figure 3 shows ROS17/2.8 cell proliferation over a period of 16 days in three conditions. The growth pattern varied according to the mechanical regimen. Maximal proliferation was obtained in TG, as compared with both FRG and DG. Peak proliferation was achieved by day 8 in TG and by day 10 in FRG. In DG, the growth rate was low all along the culture period, as compared with the two other conditions, with a peak proliferation at day 4 for 50 rpm DG and day 6 for 25 rpm DG. In each conditions, after the proliferation peak, a decreased growth rate was observed along with an increased dead cell number.

Collagen Quantification

Figure 4 showed the hydroxyproline concentration as a function of time in every condition. In FRG and TG, collagen concentration decreased similarly from day 4 to day 12, whereas in DG, this decrease was more pronounced.

Determinant of Gel Contraction

We found, in all the groups, that gel width was highly predicted by collagen concentration and cell number, $r^2 = 0.92$, $P = 0.0001$. The

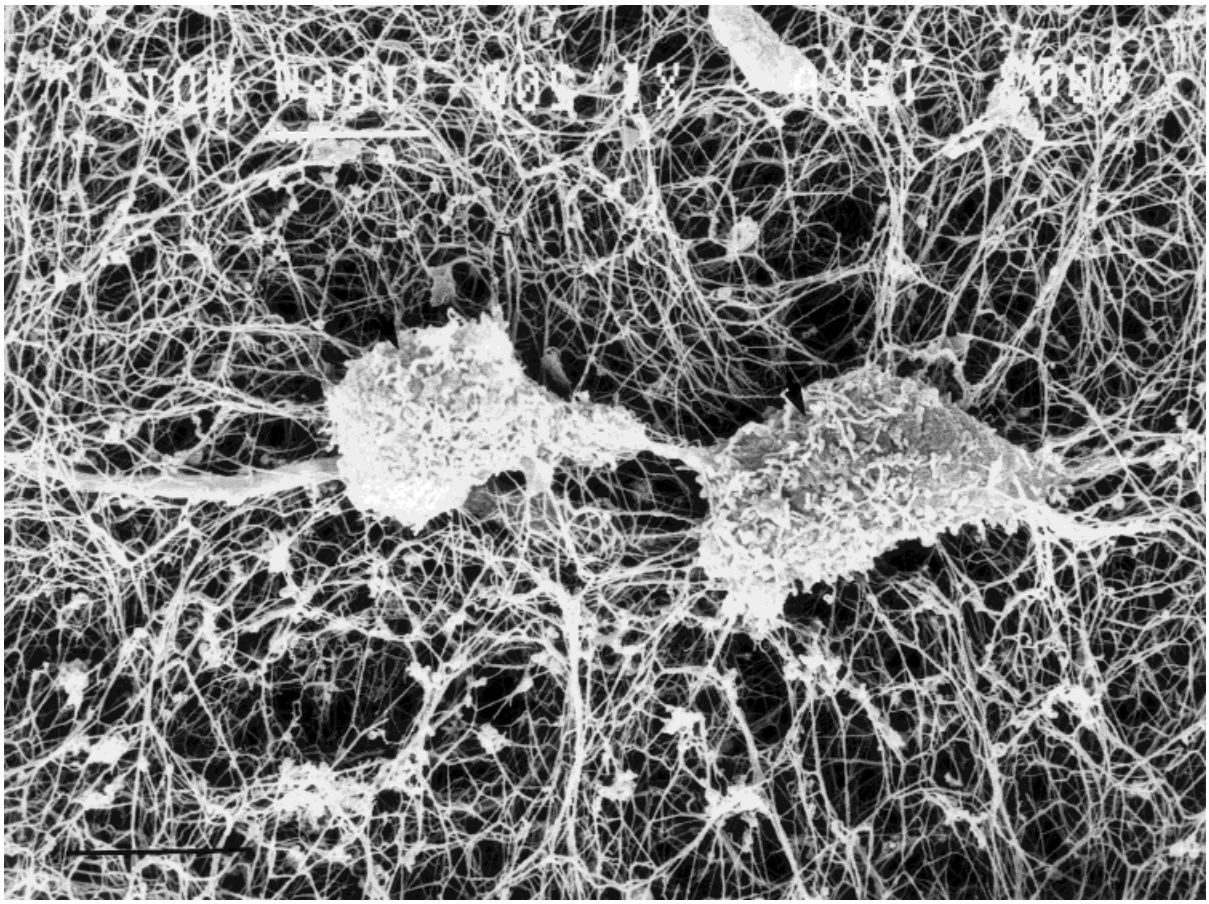

Fig. 2. SEM of isotonic control tissue (freely retracted gels [FRG]), showing cells embedded into the collagen network. Collagen fibers surrounded the cells and numerous contacts and interactions with cell body could be observed. Scale bar = 10 μm.

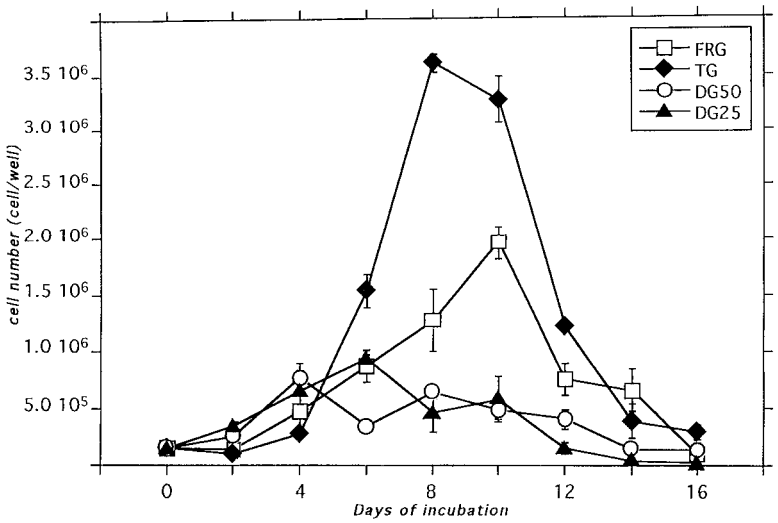

Fig. 3. Growth of the ROS17/2.8 cells. Values are means ±SD of four determinations.

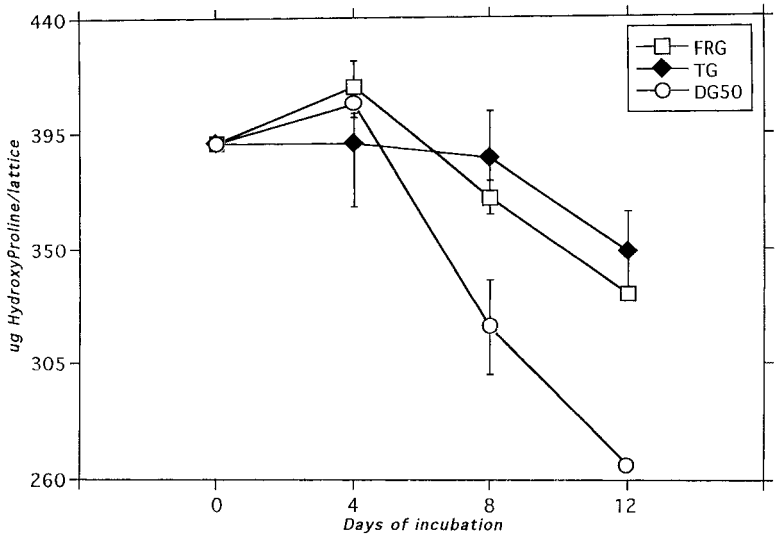

Fig. 4. Collagen concentration in collagen gels populated by ROS17/2.8 cells. Values are means ±SD of four determinations.

equation was

$$\text{Gel width} = -3.26 + 0.01\,(\text{collagen concentration}) - 0.00017\,(\text{cell number})$$

Partial *P* were 0.0001 and 0.0341, respectively. In other words, the less the lattice width, the less the collagen concentration and the more the cells.

Alkaline Phosphatase Expression in ROS17/2.8 Cells Grown in Type I Collagen Gels

Northern blot of ALP mRNA levels demonstrated differences between conditions (Fig. 5). At day 4, mRNA was detectable in each condition but was more expressed in TG versus FRG and 50 rpm DG. At day 8, we found the same differences between TG and the other conditions, but with greater amplitude. At day 12, we found the same pattern as at day 4.

Biochemical assay of enzyme activity (Fig. 6) confirmed the Northern blot analysis. Indeed, a greater ALP activity was found in TG. In DG, ALP activity remained low, as compared with the other two conditions. In FRG, ALP activity increased progressively throughout the culture. In TG, a multiphasic pattern was seen with one peak at day 4 and another one at day 16, the latest being the highest. At day 16, TG ALP was 46% higher than FRG ALP.

Osteocalcin Expression

Osteocalcin assay showed intense expression both at the beginning and at the end of culture

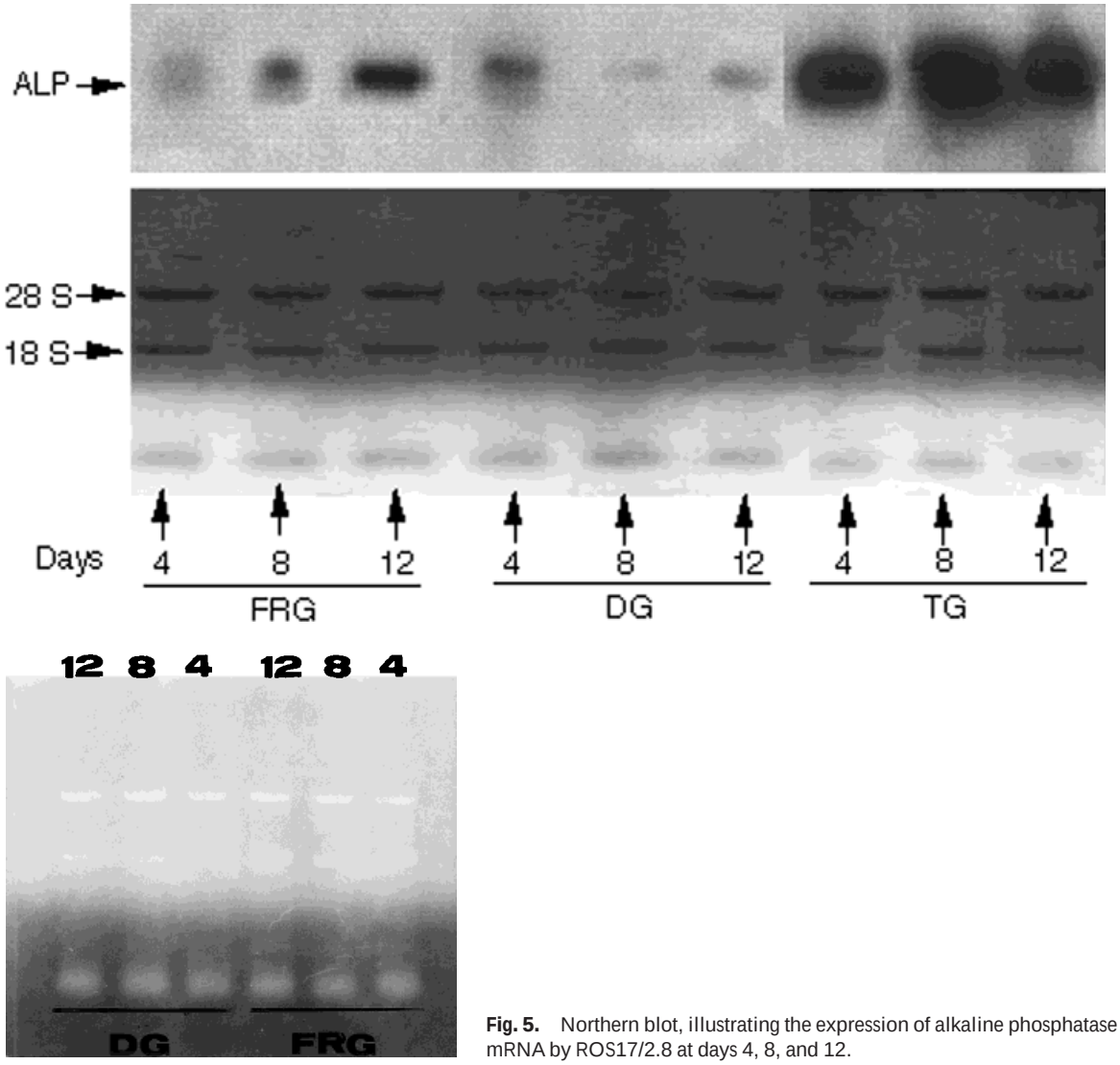

Fig. 5. Northern blot, illustrating the expression of alkaline phosphatase (ALP) mRNA by ROS17/2.8 at days 4, 8, and 12.

(Fig. 7). Expression was higher in FRG and TG at day 2 and days 16, 18 as compared with DG50. However in DG50, it was higher at day 8, 10, 12, and 14, as compared with FRG and TG.

Mineralization

Mineralization was seen with the use of TEM in each condition. The mineral crystals appeared to nucleate mainly from sites along the collagen fibers and to progress toward the fiber. Another but rarer way of mineralization consisted of nucleation from matrix vesicles. In addition, mineralization of cell debris was mainly seen at day 16, as compared with day 12 and 14 (Fig. 8).

To determine the components of the mineral, the mineralized matrix was analyzed by an energy-dispersive X-ray analyzer. The deposited minerals of the matrix were mainly composed of calcium and phosphorus. The Ca/P ratio of the mineralized areas ($1.6 \pm 0{,}04$; $n = 15$) demonstrated in all conditions of approximatively the same value as that of the hydroxyapatite crystal of bone. In gels incubated without cells, the Ca/P ratio was low (0.61), and TEM showed no mineral deposition.

To estimate mineralization rate in the three different conditions, we measured calcium concentration in the medium incubated for 24 h at 37°C every day. As early as day 15, increased mineralization was obtained in dynamic and static conditions. At the end of the experiment, it increased 263% and 94%, respectively, versus FRG.

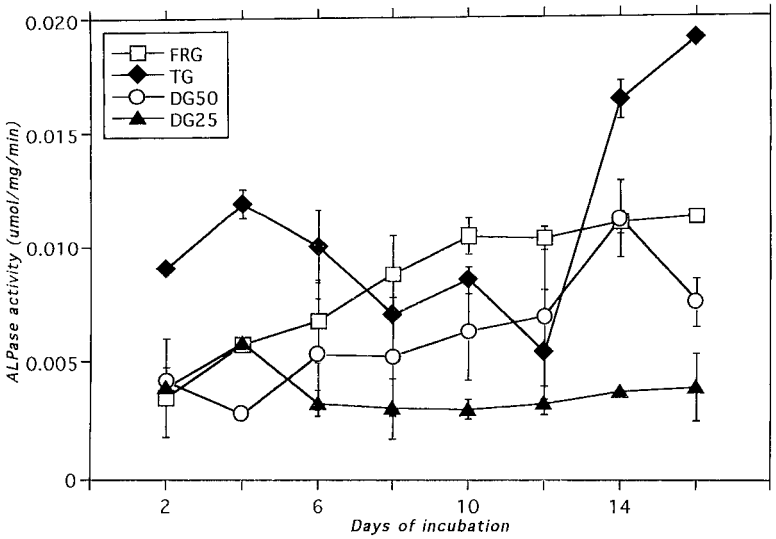

Fig. 6. Changes in alkaline phosphatase (ALP)ase activity of the ROS17/2.8 cells. Values are means ±SD of four determinations.

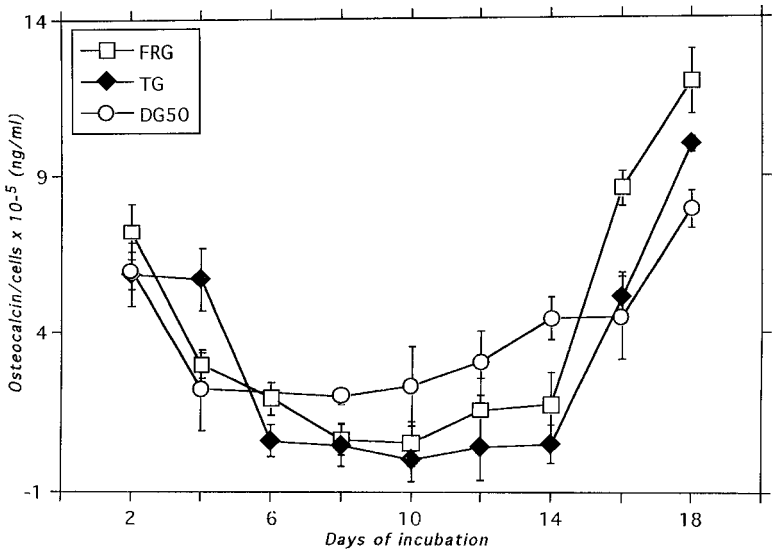

Fig. 7. Osteocalcin concentration in ROS17/2.8 cell culture medium. Values are means ±SD of four determinations.

DISCUSSION

We used a 3-D collagen type I network to study cell behavior in lattices submitted to different mechanical stress/strain regimens. We showed that, in concert with 3-D collagen matrices, static and dynamic mechanical stresses played a significant role on the phenotypic modulation of osteoblast-like cells. We provided further evidence that osteoblast-like cells have the ability to cause type I collagen gel contraction. This ability was previously described in rat alveolar bone cells cultured in collagen sponges, but not in collagen chondroitin sulfate sponges [Bouvier et al., 1990]. More recently, it has been shown that human osteosarcoma cells, MG63 and HOS, contracted collagen gels and that the transforming growth factor-β (TGF-β) mediated enhanced gel contraction was dependent on α2β1 integrin expression (known to mediate type I collagen interaction) [Riikonen et al., 1995]. Our finding contradicted the conclusion of Bellows et al. [1981] that ROS 17/2.8 cells incorporated into Vitrogen collagen did not contract the gel. However, this study lasted only 3 days, which could be an unsufficient period, as we observed that gel retraction had just began at this point.

The traction exerted collectively by a group of cells on a collagen gel was used as an assay to control the effects of mechanical regimens imposed to this 3-D system. Maximal contraction was obtained within DG (50 rpm induced more

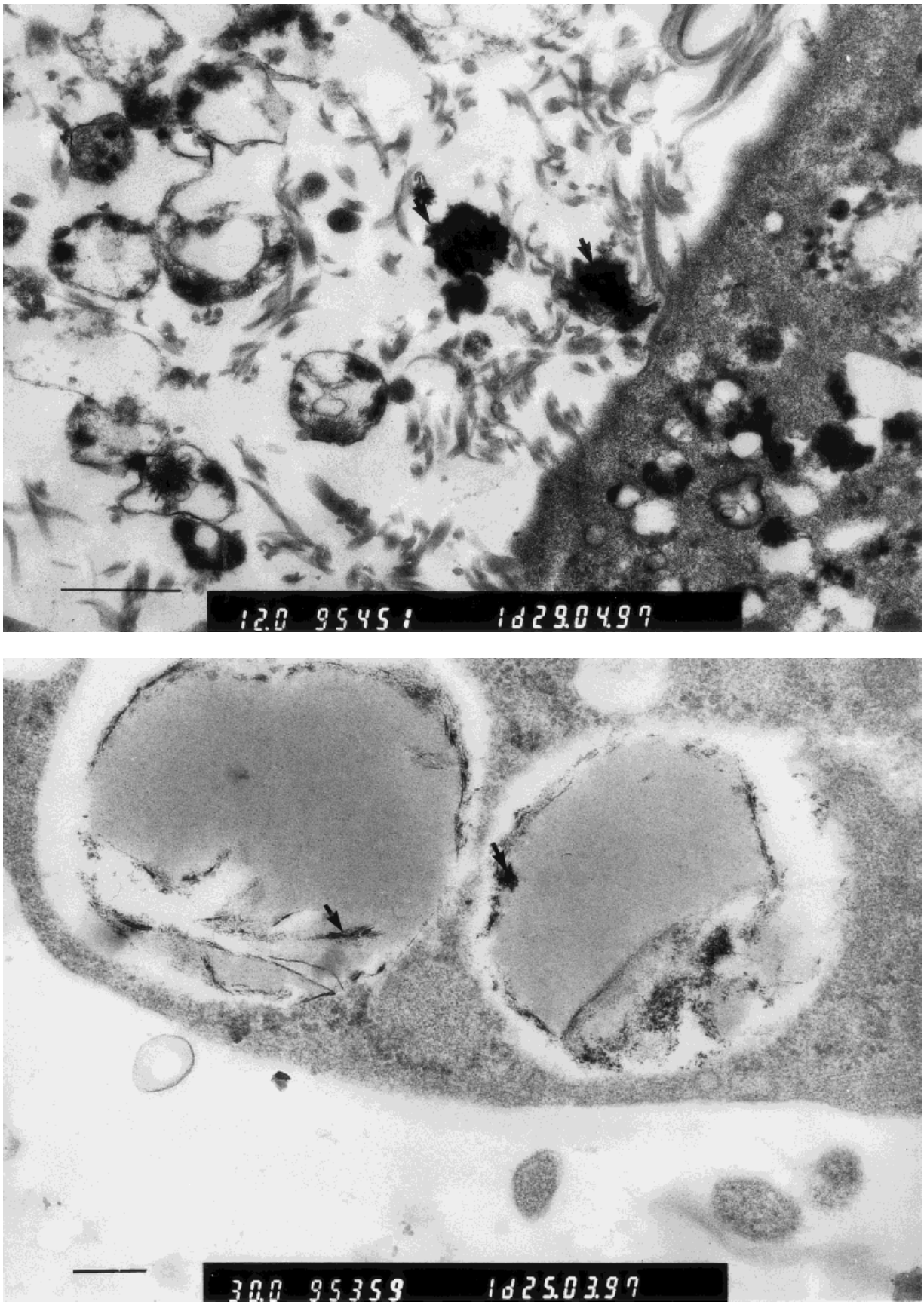

Fig. 8. TEM of mineral deposition in the cultured cells on day 16. **Top:** Spicular crystals deposited along collagen fibers. **Bottom:** Mineral may begin to grow in matrix vesicules. **Facing page:** Mineralization is also associated with cell debris. Scale bar = 1 μm.

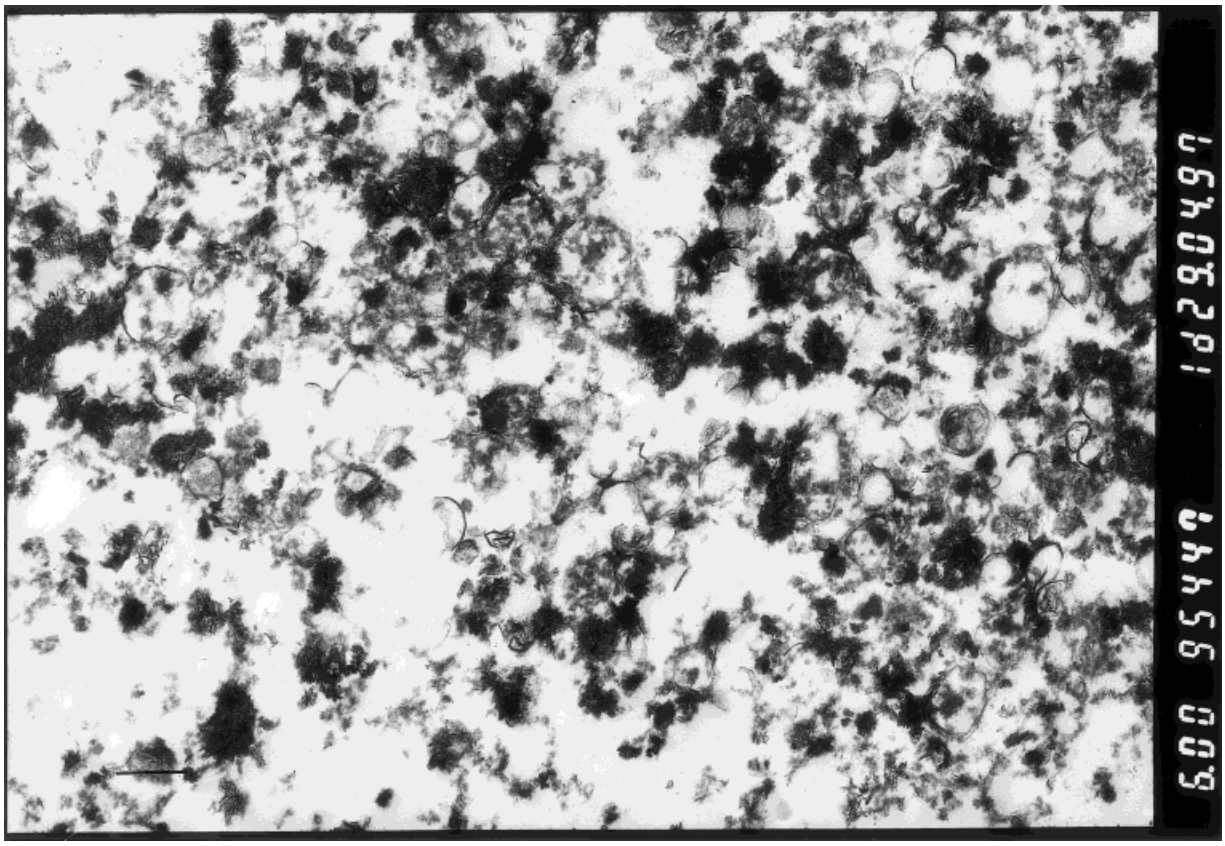

Figure 8. (Continued.)

contraction than 25 rpm), followed by FRG. The same observations were made in spherical gels (data not shown). In anchored gels (TG), a contraction was seen in the width measured at the gel centrum level, as a result of both cellular activity and longitudinal isometric tension. The contraction might reflect either different intensities of tension forces exerted by each cell on the extracellular matrix or be a consequence of increased collagen digestion measured through hydroxyproline concentration, or both. Although we did not measure the collagenase production, our results suggested mixed responses. Indeed, gel dimension was predicted positively by collagen concentration and negatively, and to a lesser extent, by cell number. In DG, where the proliferation was minimal throughout the experiment, gel contracted more strongly than in other conditions. Thus, despite the decrease in the amount of collagen to be contracted with time, the contraction potential per cell might be higher in DG versus FRG. Indeed, by day 8, the collagen amount was only 14% less, whereas cell number and gel surface were about 50% less in 50 rpm DG gels versus FRG. Morphologically, DG cells appeared rounder and larger, as compared with control gel cells. The actin stress fibers in larger cells might be able to generate higher intracellular forces, and subsequently higher extracellular tractional forces, even though fewer cellular links between cell aggregates were seen in DG, as compared with other conditions. In fact, it was previously shown that tractional forces could be exerted without direct cell-cell contacts, through the collagen bundles (Klebe et al., 1989).

In control gels (FRG), cells were spherical within aggregates and bipolarly elongated in multidirectional branching between aggregates. At the ultrastructural level, cells were found to insert into the collagen network; in some cases, dense collagen fiber bundles were seen close to the cellular body. This phenomenon was even more obvious in TG, where mechanical tension was mainly vectorial and directed between opposing edges; fibers were aligned parallel to the direction of stretch. Therefore, interaction between matrix and cells appears to have led to both collagen fibers and osteoblastic cell orientations. This primarily longitudinal orientation

did not impede lateral links between cells, leading to contraction in the centrum of the gel. The parallel alignment of the long axis of cells in TG to the orientation of collagen fibers can be explained by the fact that integrin receptors mediated the interaction of cells with both collagen and fibronectin. As the location of actin cables in the cytoplasm coincides with fibronectin and collagen fibers on the cell surface [Horowitz et al., 1986], the integrin receptor may serve as an intermediary in imposing the prevailing orientation of collagen on cytoplasmic actin cables. The alignment of actin cables with collagen fibers would then serve to amplify the mechanical forces that govern the orientation of collagen fibers. This assumption might have very important implications in vivo at the osteoid lamellar level, where one of the most important, although not well known, osteoblast functions might be to arrange collagen cables in the tissue to provide maximum strength to the bone for a minimum amount of material.

This highly sophisticated organization might depend on mechanical strain. We effectively showed that osteoblast function responds to changes in mechanical environment. Indeed, we showed that the osteoblastic phenotype modulated by collagen matrix contraction differed dramatically depending on the mechanical regimen applied. As compared with FRG, cell proliferation was stimulated in TG and inhibited in DG. Nevertheless, in each case, the exponential proliferation phase coincided with the maximum gel contraction phase. A marked decline in cell growth was observed when gel contraction slowed or stopped. In this phase, cell death was noted, on the basis of both dye exclusion and electron micrographs. This could be attributable to contraction-related confinement. It is usually admitted that primary cells cultured in collagen gels exhibited slower growth, as compared with monolayers [Talley-Ronsholdt et al., 1995]. However, we calculated doubling population time during exponential phases in each condition and found 13 h, 11 h, 19 and 21 h in FRG, TG, and 25 and 50 rpm DG, respectively, whereas in monolayers it was 35 h (data not shown). Thus 3-D culture conditions stimulated proliferation of osteosarcoma cells, as opposed to primary cells.

Despite the increased proliferation rate, the differentiation also appeared to be stimulated, although differently, according to the mechanical regimen. In the four but one (DG25) experimental condition, ALP activity was higher at the end of the culture, with the highest level seen in TG, as compared with the other conditions. The results obtained from mRNA were in accordance with enzymatic activity and showed high levels in TG, followed by FRG and DG by the end of the culture period. Calcium content increased as early as day 15 in DG50 and TG, with the evolution similar in these two conditions up to day 16. Calcium content then increased dramatically in DG50 gels, as compared with TG. In FRG, a slight increase was seen at the end of the experiment. As a whole, when compared with FRG, the static regimen in TG appeared to promote both proliferation rate, protein production, and calcium deposition, whereas the dynamic regimen (DG50) did stimulate osteocalcin production and calcium deposition, although to a lesser extent than occurred with TG, but inhibited cell growth and ALP activity. Interestingly, for ALP in TG and for osteocalcin production in every condition, a triphasic pattern was seen, characterized by high levels of both proteins, at initiation of the culture, cells could then dedifferentiate, with their activities more involved in metabolism related to proliferation, secondarily permitting cell differentiation expression with levels surpassing those of the initial phase. These 3-D profiles appeared different from the usual profile of differentiation observed in osteoblastic cells in conventional 2-D cultures, characterized by the expression of genes usually seen in the early (collagen, ALP) or late (osteocalcin) phases of maturation [Stein et al., 1989; Stein and Lian, 1995]. We interpreted initial increases in the ALP activity of TG and in osteocalcin in every condition by the fact that cells seeded will differentiate at once as a result of the combined effects of 3-D environment and collagen type I. Several studies have indicated that type I collagen affects the expression of the bone cell phenotype, primarily ALP activity. Lynch et al. [1995] showed that genes normally expressed at high levels on plastic during the initial proliferation period are down-regulated in fetal rat calvarial cells seeded onto collagen type I films, whereas genes normally expressed at maximal levels during the postproliferative period were up-regulated severalfold very early. Masi et al. [1992] showed that Saos-2 cells colonized collagen sponges. In this 3-D network, they were able to synthesize osteocalcin. Our results showed that the collagen type I

network permitted the phenotypic expression of osteocalcin from seeded cells, a property specific to functional osteoblasts [Lian et al., 1998], before they actively divided. It is conceivable that stimulation of the osteoblastic phenotype by collagen type I is secondary to the interaction of specific cell surface receptors with this 3-D network.

Thus, differential influences of mechanical regimen were seen in the proliferative profile and ALP activities, both of which are stimulated in TG, as compared with other conditions. We were the first to report matrix mineralization in osteosarcoma-derived cell lines grown within collagen type I gels. The Ca/P ratio of mineralized areas showed the same value (1.6 ± 0.04) as that of hydroxyapatite. It is known that, in denatured collagen, osteosarcoma cell lines such as TE-85 or SAOS-2 [Heermeier et al., 1995] did not build up mineralizing tissue, even in a 3-D environment. Ultrastructural studies performed at the end of the culture period showed that mineralization within the matrix is uniform. Furthermore, matrix mineralized by a different process. The most important process was the deposition of crystals along the collagen fibers, rarely seen in vitro [Gotoh et al., 1990] but shown in vivo. The same type of mineralization was reported by Herbert et al. [1997] in osteoblast-like cells from newborn rat calvaria collected by placing glass fragments onto the endocranial surface of periosteum-free bone. A second, and more rare, process was represented by extracellular vesicule-like structures that are commonly reported in in vitro studies and in epiphyseal cartilage in vivo [Bonucci, 1992]. A third process was the mineralization of cell debris, which might be the consequence of a calcification through the efflux of calcium from dead cells [Trump et al., 1981].

In conclusion, this study provided evidence that the entire process of differentiation, including mineralization, could be obtained in a 3-D collagen type I network. Furthermore, the sequence of events including cell proliferation and the amount of protein deposition and calcium accumulation were strongly dependent on the mechanical environment. The gel contraction velocity that differed according to the stress/strain applied offered an index representing extracellular matrix remodeling cell ability, providing a tool with which to study how various chemical and physical factors may modulate this ability. TG should better mimic an in vivo-like ressembling osteoid tissue in which the arrangement of the organic matrix on the mineralized bony tissue is clearly one of osteoblast function.

ACKNOWLEDGEMENTS

The authors are grateful for the cooperation and assistance of Isabelle Anselme-Bertrand and Paul Jouffrey, Centre de Microscopie électronique Stéphanois.

REFERENCES

Bellows CG, Melcher AH, Aubin JE. 1981. Contraction and organization of collagen gels by cells cultured from periodontal ligament, gingiva and bone suggest functional differences between cell types. J Cell Sci 50:299–314.

Bellows CG, Aubin JE, Heershe JNM, Antosz ME. 1986. Mineralized bone nodules formed in vitro from enzymatically released rat calvaria cell population. Calcif Tissue Int 38:143–154.

Benayahu D, Kletter Y, Zipori D, Wientroub S. 1989. Bone marrow-derived stromal cell line expressing osteoblastic phenotype in-vitro and osteogenic capacity in vivo. J Cell Physiol 140:1–7.

Benayahu D, Kompier R, Shamay A, Kadouri A, Zipori D, Wientroub S. 1994. Mineralization of marrow-stromal osteoblasts MBA-15 on three-dimensional carriers. Calcif Tissue Int 55:120–127.

Bonucci E. 1992. Comments on the ultrastructural morphology of the calcification process: an attempt to reconcile matrix vesicules, collagen fibrils and cristal ghosts. Bone Miner 17:219–222.

Bouvier M, Couble ML, Hartmann DJ, Gauthier JP, Magloire H. 1990. Ultrastructural and immunocytochemical study of bone-derived cells cultured in three-dimensional matrices: influence of chondroitin-4 sulfate on mineralisation. Differentiation 45:128–137.

Bradford MM. 1976. A rapid and sensitive method for the quantification of microgram quantities of protein utilizing the principle of protein dye binding. Anal Biochem 72:248–254.

Caillot-Augusseau A, Pernod J, Vergely N, Soler C, Clavier A, Benabdesselam F. 1996. L'ostécalcine: un marqueur de la formation osseuse. Aspects méthodologiques. Immunoanal Biol Spec 11:95–103.

Casser-Bette M, Murray AB, Closs EI, Erfle V, Schmidt J. 1990. Bone formation by osteoblast-like cells in a three-dimensional cell culture. Calcif Tissue Int 46:46–56.

Chomczynski P, Sacchi N. 1987. Single-step method of RNA isolation by acid guanidium thiocyanate-phenol-chloroform extraction. Anal Biochem 162:156–159.

Duncan RL, Turner CH. 1995. Mechanotransduction and the functional response of bone to mechanical strain. Calcif Tissue Int 57:344–358.

Ernest M, Froesch ER. 1987. Osteoblast-like cells in a serum-free methyl cellulose medium form colonies: effects of insulin and insulin-like growth factor I. Calcif Tissue Int 410:27–34.

Forwood MR, Turner CH. 1995. Skeletal adaptations to mechanical usage: results from tibial loading studies in rats. Bone 17:197S–205S.

Gotoh Y, Hiraiwa K, Nagayama M. 1990. In vitro mineralization of osteoblastic cells derived from human bone. Bone Miner 8:239–250.

Granet C, Laroche N, Vico L, Alexandre C, Lafage-Proust MH. 1998. Rotating-wall vessels, promising bioreactors for osteoblastic cell culture: comparison with other 3D conditions. Cell Eng 3:513–519.

Guignandon A, Genty C, Vico L, Lafage-Proust MH, Palle S, Alexandre C. 1997a. Demonstration of feasibility of automated osteoblastic line culture in space flight. Bone 20:109–116.

Guignandon A, Usson Y, Laroche N, Lafage-Proust MH, Sabido O, Alexandre C, Vico L. 1997b. Effects of intermittent or continuous gravitational stress on cell-matrix adhesion. Quantitative analysis of focal contacts in osteoblastic cells ROS 17/2.8. Exp Cell Res 236:66–75.

Heermeier K, Spanner M, Träger J, Gradinger R, Schmidt J. 1995. Bone formation of human osteoblast-like cells in a three-dimensional cell culture: an in vitro model for studies of skeletal disorders. Cells Mater 5:309–321.

Horowitz A, Duggan K, Buck C, Beckerle MC, Burridge K. 1986. Interaction of plasma membrane fibronectin receptor with talin-alpha transmembrane linkage. Nature 320: 531–533.

Klebe RJ, Caldwell H, Milan S. 1989. Cells transmit spatial information by orienting collagen fibers. Matrix 9:451–458.

Lian JB, Stein GS, Stein JL, van Wijnen AJ. 1998. Osteocalcin gene promoter: unlocking the secrets for regulation of osteoblast growth and differentiation. J Cell Biochem Suppl 30–31:62–72.

Lynch MP, Stein JL, Stein GS, Lian JB. 1995. The influence of type I collagen on the development and maintenance of the osteoblast phenotype in primary and passaged rat calvarial osteoblasts: modification of expression of genes supporting cell growth, adhesion, and extracellular matrix mineralization. Exp Cell Res 216:35–45.

Majeska RJ, Rodan SB, Rodan GA. 1980. Parathyroidhormone responsive clonal cell lines from rat osteosarcoma. Endocrinology 107:1494–1503.

Majmudar G, Bole D, Goldstein SA, Bonadio J. 1991. Bone cell culture in a three-dimensional polymer bead stabilizes the differentiated phenotype and provides evidence that osteoblastic cells synthesize type III collagen and fibronectin. J Bone Miner Res 8:869–881.

Masi L, Franchi A, Santucci M, Danielli D, Arganini L, Giannone V, Formigli L, Benvenuti S, Tanini A, Begh F, Mian M, Brandi ML. 1992. Adhesion, growth, and matrix production by osteoblasts on collagen substrata. Calcif Tissue Int 51:202–212.

Riikonen T, Koivisto L, Vihinen P, Heino J. 1995. Transforming growth factor-β regulates collagen gel contraction by increasing α2β1 integrin expression in osteogenic cells. J Biol Chem 20:376–382.

Rubin CT, Lanyon LE. 1985. Regulation of bone mass by mechanical strain magnitude. Calcif Tissue Int 37:411–417.

Stegeman H. 1958. Microbes timmung von hydroxyprolin mit chloranin T und p. dimethylaminobenzaldehyd. Z Physiol Chem 311:41–45.

Stein GS, Lian JB. 1995. Molecular mechanisms mediating proliferation-differentiation interrelationships during progressive development of the osteoblast phenotype: update 1995. Endocr Rev 4:290–297.

Stein GS, Lian JB, Gerstenfield LG, Shalhoub V, Aronow M, Owen T, Marckose E. 1989. The onset and progression of osteoblast differentiation is functionally related to cellular proliferation. Connect Tissue Res 20:2–13.

Sudo H, Kodama HA, Amagai Y, Itakura Y, Yamamoto S. 1986. Mineralized tissue formation by MC3T3-E1 osteogenic cells embedded in three-dimensional gel-matrix. In: Ali SY, editor. Cell mediated calcification and matrix vesicules. New York: Elsevier Science. p 291–296.

Talley-Ronsholdt DJ, Lajiess E, Nagodawithana K. 1995. Transforming growth factor-beta inhibition of mineralization by neonatal rat osteoblasts in monolayer and collagen gel culture. In Vitro Cell Dev Biol 31:274–282.

Trump BF, Berezesky IK, Osornio-Vargas AR. 1981. Cell death and the disease process. The role of calcium. In: Bowen ID, Lockshin RA, editors. Cell death in biology and pathology. London: Chapman & Hall. p 209–242.

Vico L, Lafage MH, Alexandre C. 1998. Effects of gravitational changes on the bone system in vitro and in vivo. Bone 22:95S–100S.